GCAGS JOURNAL
A Publication of the Gulf Coast Association of Geological Societies
www.gcags.org

Comparative Stratigraphy of the Eagle Ford Group Strata in Lozier Canyon and Antonio Creek, Terrell County, Texas

Rand D. Gardner[1], Michael C. Pope[1], Matthew P. Wehner[1], and Art D. Donovan[2]

[1]*Department of Geology and Geophysics, Texas A&M University, MS 3115, College Station, Texas 77843, U.S.A.*

[2]*BP, 501 Westlake Park Blvd., Houston, Texas 77079, U.S.A.*

ABSTRACT

High-resolution correlation of individual beds in the Eagle Ford Group over several miles in Lozier Canyon and Antonio Creek in Terrell County, Texas, documents the lateral variation of these strata on the scale of a horizontal well. Physical tracing of the beds, hand-held spectral gamma-ray scintillometer profiles, and the examination of polished hand samples and thin sections were used to correlate Eagle Ford Group strata across the study area. Five distinct lithostratigraphic units, termed A–E from the base up, and their sub-units, are laterally continuous laterally continuous over several miles in terms of thickness, lithology, and spectral gamma ray response. The lateral continuity of these units suggests that there was little overall difference in depositional environment across the study area; however, there are subtle differences in thickness and sedimentary structures. Unit A has the largest difference in thickness (7%) suggesting higher sediment supply in the southeast of the study area. Sedimentary structures and bed morphology of several beds in unit B vary over a 4 mi (6 km) interval suggesting higher sediment supply in the southeast of the study area. Differences in paleobathymetry at the commencement of Eagle Ford deposition may have contributed to the lateral variation in units A and B. Geochemical data and trace fossil abundance suggest primarily anoxic bottom water conditions in the Lower Eagle Ford formation and oxic conditions in the Upper Eagle Ford formation. Laterally extensive bedding plane exposures in Antonio Creek reveal 3D views of macrofossils and the morphology of bedforms which were previously only described from 2D outcrops. Sedimentary structures suggest that units A, C, D, and E were deposited within storm wave base and deposition of unit B was episodically within storm wave base. This study documents the horizontal variability (e.g., thickness, composition, sedimentary structures, and gamma ray response) of the Eagle Ford Group strata in Lozier Canyon and Antonio Creek, West Texas.

INTRODUCTION

The development of unconventional mudstone reservoirs like the Eagle Ford, Gothic, Marcellus, Utica, Haynesville, and Woodford formations and similar "shale plays" illustrate the need of understanding and predicting horizontal variability in mudstone reservoirs on the scale of a single lateral well. The horizontal component of a typical Eagle Ford well is 4500 ft (1400 m) long and contains 15 hydraulic fracture stages. The optimization of a horizontal drilling program depends on positioning and completing the lateral portion of a well in a way that maximizes revenue over the duration of well production. The outcrops here provide an opportunity to study lateral variability on this scale.

Manuscript received April 9, 2013; revised manuscript received June 19, 2013; manuscript accepted July 1, 2013.

GCAGS Journal, v. 2 (2013), p. 42–52.

The Eagle Ford Group can be studied at numerous sites within Lozier Canyon and its side tributaries, such as Antonio Creek, in Terrell County Texas (Fig. 1). Based on work at the initial Lozier Canyon research site 1 (Fig. 1) in Lozier Canyon, Donovan et al. (2012) divided the Eagle Ford Group into four depositional sequences, and illustrated the complex vertical variability of these strata. Furthermore, using petrophysical, biostratigraphic, and geochemical data, they suggested that the sequences and surfaces defined at the Lozier Canyon 1 site could be correlated into the subsurface and used to explain the thickness and facies distribution of the Eagle Ford unconventional reservoirs in South Texas. This work, however, did not address the lateral continuity or variability of individual beds within each of the four sequences defined within the Eagle Ford.

Eagle Ford outcrops in Lozier Canyon proper occur as semi-continuous cut-bank exposures along an approximate 8 mi (13 km) stretch from U.S. Highway 90 to the U.S.-Mexico international border along the Rio Grande River. Typically, each of these cut-bank exposures is 1000's of ft (100's of m) long and 100's of ft (10's of m) high, providing good cross-sectional (2D) perspectives of bedding within the Eagle Ford. Recently, a new

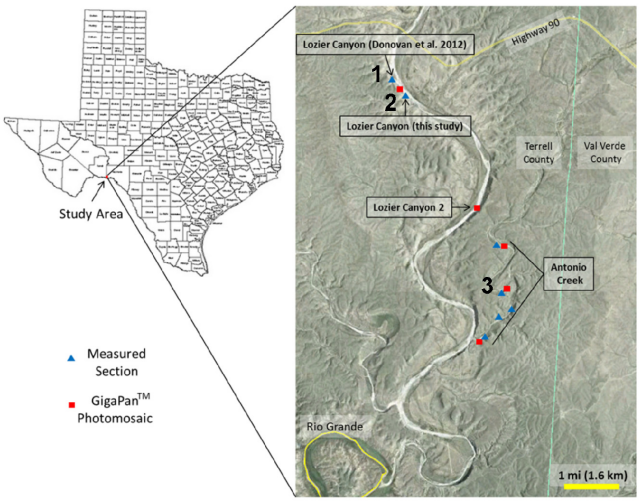

Figure 1. Map of the study area showing the location of measured sections (blue triangles) and annotated Gigapan™ photomosaics (red squares) of Lozier Canyon and Antonio Creek.

research site (#3) at Antonio Creek, a tributary to Lozier Canyon (Fig. 1), was studied. At this site, canyon floor exposures provide a unique opportunity to also examine bedding plane exposures of most of the Eagle Ford strata providing a unique opportunity to obtain a 3D perspective of the bedforms and fractures sets. Due to climate and physiography, the Eagle Ford outcrops of West Texas provide a unique opportunity to study outcrops of a prolific unconventional mudstone reservoir in the subsurface of South Texas.

GEOLOGIC SETTING

Sloss (1963) designated the Middle Jurassic through latest Cretaceous succession of North America as his unconformity-bounded Zuni Sequence, with the Cenomanian through Turonian portion of the Cretaceous occurring at or near the maximum flooding surface of this first-order sequence. It was during this major marine incursion of the Zuni Sequence in the Cretaceous, that the Eagle Ford and equivalent (Woodbine) strata were deposited across Texas. Over much of Texas, a well-developed carbonate platform developed during the Early Cretaceous and earliest Late Cretaceous (Fig. 2). Hill (1887) referred to this carbonate-prone succession as the Comanche Series and named the overlying more clastic-prone strata the Gulfian Series. Within South and West Texas, the Buda/Eagle Ford contact marks the boundary between Hill's (1887) Comanche and Gulfian series (Fig. 3).

A well-developed carbonate platform, referred to as the Comanche Platform, developed during the Albian and Early Cenomanian across much of Central Texas. In South and West Texas, the platform-margin reef buildups on the Comanche Platform are commonly referred to as the Stuart City and Santa Elena trends. As illustrated on Figure 4, these reef buildups greatly influenced the inherited physiography of the overlying Eagle Ford succession.

PREVIOUS WORK

The Eagle Ford outcrops of West Texas, which are also referred to as the Boquillas Formation, have been studied by a number of previous workers. Key works on the stratigraphy of the Eagle Ford include Hazzard (1959), Freeman (1961, 1968), and Pessagno (1969). Many aspects of the lithologies and sedimentology were covered by Trevino (1988), as well as Lock and Peschier (2006). Key biostratigraphic papers include Pessagno (1969) and Smith (1973). Donovan and Staerker (2010) utilized much of this previous work to subdivide the vertical facies succession observed in these outcrops into five (5) basic units, which they termed A to E from the base up. This work was expanded and refined based on additional lithologic, biostratigraphic, geochemical, sedimentological, and petrophysical properties of these strata (Donovan et al, 2012), to subdivide further the 5 basic lithologic units into sub-units (16 total). These units and sub-units were then used to define four distinct depositional sequences within the Eagle Ford (K63, K64, K65, and K70), each of which the authors suggested could be mapped as distinct members.

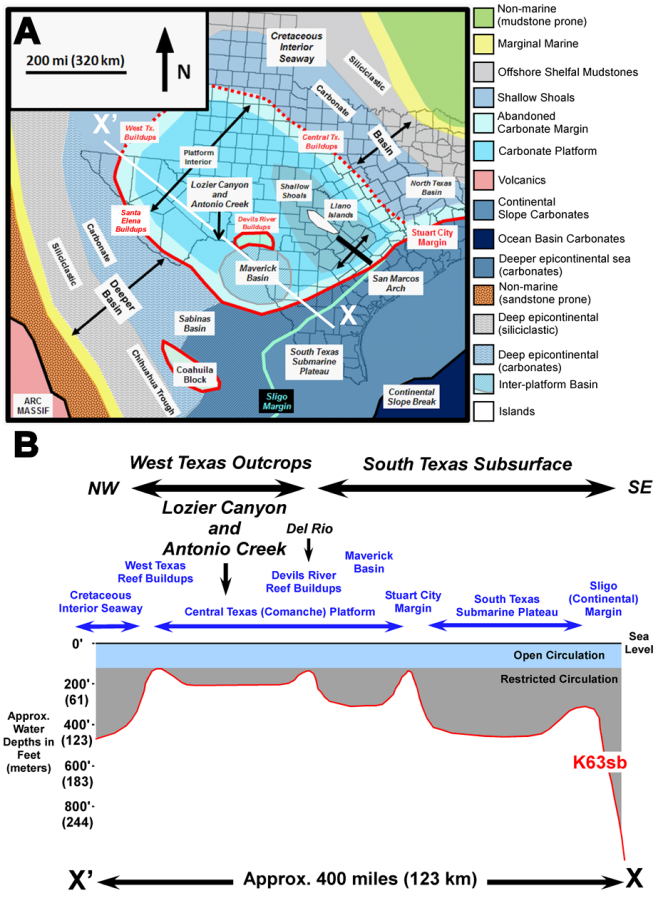

Figure 2. (A) Generalized paleogeographic map of the Comanche Platform during the late Cenomanian. (B) Generalized cross section from X to X' (modified after Donovan and Staerker, 2010).

METHODS

This study of the Eagle Ford Group strata in Lozier Canyon and Antonio Creek includes both field work and petrographic analysis. A composite section was measured and described in each canyon in 2012. Carbonate rocks were classified using Dunham's classification (1962) and sedimentary structures were described following Campbell's classification (1967). Measured sections include descriptions of bed lithology, color, thickness, fossils, ichnofabric index after Droser and Bottjer (1986), and sedimentary structures. Wave ripples and current ripples share many characteristics and can look very similar. In this study, the criteria in Table 1 were followed to distinguish between these sedimentary structures in this study and maintain consistency. Hand samples were collected every 2–3 ft (60–90 cm) at the Lozier Canyon section and every ft (30 cm) in the Antonio Creek section. A Gigapan™ system was used to photograph Eagle Ford Group outcrops and create photomosaics to document the variation of individual beds across 1000's of ft (100's of m) of outcrop. A hand-held gamma-ray scintillometer collected spectral gamma-ray (SGR) values at 1 ft (30 cm) intervals from each measured section. Slabbed and polished hand samples from the

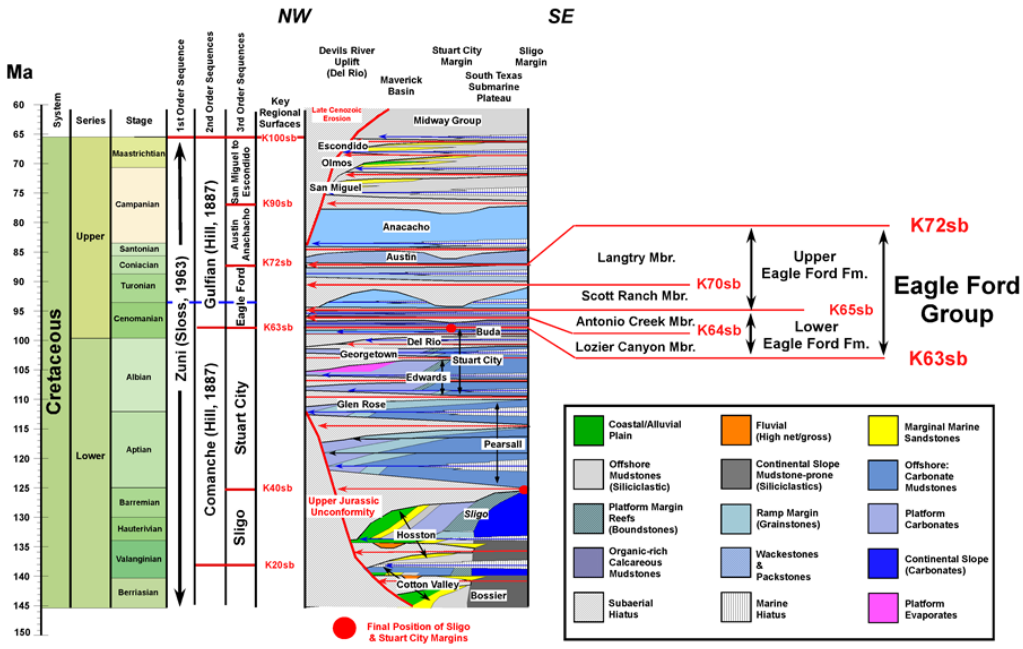

Figure 3. Cretaceous chronostratigraphy of South Texas (modified after Donovan et al., 2012).

outcrop were described with a hand lense and a binocular microscope. Sixty-seven 2x3 in (5x7.5 cm) thin sections were described with plain light and cathodoluminescent microscopy.

The 5 basic lithostratigraphic units (A–E) and 16 sub-units, defined by Donovan et al. (2012) were identified on the sections measured in this study and are illustrated on Figure 4. It should also be noted, that the Lozier Canyon measured section in this study (Figs. 1 and 3) is located about 3000 ft (1 km) from the section measured in Lozier Canyon by Donovan et al. (2012) along the same cut-bank outcrop.

Sources of Error

There are several variables that may have affected the SGR readings collected during this study. Portions of the SGR data in each section were collected on different trips and during different climatic conditions, which affect the amount of background radiation detected by the instrument, the RS230. Abrupt changes in temperature can also affect the stability of the instrument (RS230 User Manual). A 1 ft (30 cm) sampling interval was used in both outcrops; beds less than 1 ft (30 cm) thick that were sampled in one canyon may not have been sampled at the other locality.

RESULTS

Lithologic Units

As defined by Donovan et al. (2012), the Eagle Ford Group in this study area is unconformably bounded succession, which overlies the Buda Formation and is in turn overlain by the Austin Chalk. Key surfaces, as well as bentonite beds, provide a chronostratigraphic framework for correlating individual beds between Lozier Canyon and Antonio Creek with a high degree of confidence (Fig. 4; Table 2). This framework also facilitates the location of unit boundaries and beds on Gigapan photomosaics (Fig. 5A).

The five informal lithostratigraphic units (A–E) of the Eagle Ford Group are outlined below and described in detail in Table 3. Unit A consists of about 20 ft (6 m) of hummocky and swaley cross-stratified skeletal grainstone (Fig. 6A) interbedded with very dark gray calcareous mudstone. Few bentonites occur in this unit. Unit B consists of approximately 75 ft (23 m) of very dark gray calcareous mudstone (Fig. 6B) interbedded with thin beds of skeletal packstone (Fig. 6C). Multiple bentonite beds occur within unit B, especially in its upper part. Unit C consists of about 40 ft (12 m) of skeletal wackestone-packstone interbedded with dark gray calcareous mudstone. Thicker bentonite beds are conspicuously absent in unit C. Unit D contains approximately 20 ft (6 m) of nodular skeletal packstone (Fig. 6D) interbedded with medium gray calcareous mudstone. There some thin bentonites in unit D and one deformed zone. Unit E consists of about 25 ft (8 m) of wave rippled skeletal packstone interbedded with medium gray calcareous mudstone. Two bentonite marker beds and at least two deformed zones occur in unit E.

Lateral Correlations

Key surfaces and individual beds were traced across each outcrop and correlated between the two composite sections (Fig. 7). The thickness of sub-units typically varies by less than a few ft across the study area (Table 4). Thicker bentonites are the most correlative beds, however some resistant beds and bedsets are also correlative. The lateral continuity of several these beds is described below. All footage notes in the proceeding sections and figures are in height above the Buda Formation–Eagle Ford Group contact.

Lower Eagle Ford

Four thin (<2 in or <3 cm thick) bentonite beds and four thicker, laterally continuous skeletal grainstone bedsets are laterally continous across the study area (Fig. 5C). These grainstone bedsets mark the boundaries of the four sub-units. Most beds in unit A are laterally discontinous and pinch out or are scoured out over 10's of ft (several m), but the beds within each sub-unit have similar thickness and sedimentary structures across the study area. A zone of laterally continuous deformed bedding in

Table 1. Defining characteristics of wave versus current sedimentary structures.

Wave	Current
Symmetrical and asymmetrical	Asymmetrical
Convex up with bi directional downlap	Rarely convex up, usually onlap on one side
Hummocks	Trough cross stratification
Swales	Starved ripples
Laminae flatten upwards	Laminae flatten downwards

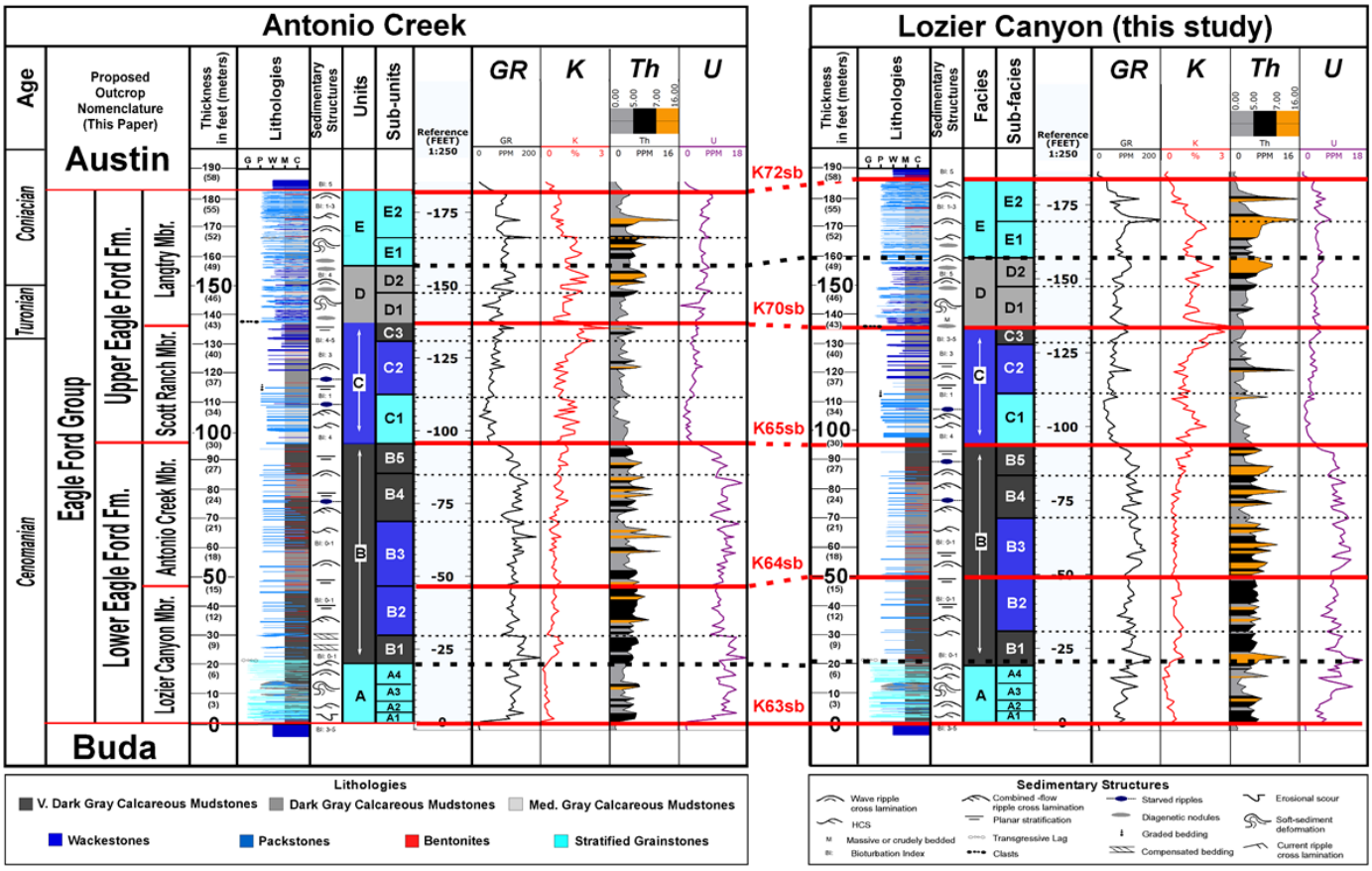

Figure 4. Correlated lithology and spectral gamma ray logs between Lozier Canyon and Antonio Creek. Names are proposed for two previously unamed members, now known as the Lozier Canyon and Scott Ranch members for the locality of the best outcrops for each interval. The Antonio Creek (previously known as the Middle Shale member) is so named for the laterally continuous exposures in that locality.

Table 2. Significant chronostratigraphic surfaces. The location (in ft and m above the Buda Limestone) of laterally continuous unit boundaries and marker bentonites. Listed under the Unit Boundaries section is a column showing the percent difference in thickness in each unit between Lozier Canyon and Antonio Creek.

Unit Boundaries				Marker Bentonites	
Boundary	**Lozier Canyon**	**Antonio Creek**	**ΔThickness**	**Lozier Canyon**	**Antonio Creek**
A–B	20.5 ft (6.2 m)	22.0 ft (6.7 m)	7.3%	172.5 ft (53 m)	176.6 ft (53.8 m)
B–C	95.0 ft (28.9 m)	96.0 ft (29.3 m)	0.7%	166.5 ft (51.3 m)	170.0 ft (51.8 m)
C–D	135.5 ft (41.3 m)	136.5 ft (41.6 m)	0.0%	77.8 ft (23.7 m)	78.0 ft (23.8 m)
D–E	156.5 ft (47.7 m)	156.5 ft (47.7 m)	4.8%	63.5 ft (19.4 m)	65.3 ft (19.9 m)
E–Austin	183.5.0 ft (55.9 m)	182.5 ft (55.6 m)	3.7%	58.5 ft (17.8 m)	59.8 ft (18.2 m)

sub-unit A3 ranges in thickness from 2–5 ft (0.6–1.5 m). Soft sediment deformation in the form of load casts, convolute bedding, and fluid escape structures are common. Portions of the skeletal grainstones are internally homogenized and lack primary sedimentary structures. An additional, separate zone of deformed bedding occurs locally in Antonio Creek at 9 ft (2.7 m). This contorted zone is discontinuous, less than 1 ft (30 cm) thick and commonly less than 10 ft (3 m) wide in several locations across a 1000 ft (300 m) unit A in Antonio Creek and is not visible elsewhere. In sub-unit A4, a zone of shell lags containing oysters, bivalves, shark teeth, fish bones, and phosphatic grains occurs across the study area.

Unit B is characterized by organic rich calcareous mudstone interbedded with about 15% interbedded skeletal packstone beds and 5% bentonite beds by volume. Thicker bentonite and skeletal packstone beds within unit B are laterally continous across the study area. Erosional surfaces are common within the calcareous mudstone facies and thinner bentonites are locally scoured out. Intervals of closely spaced thinner bentonite beds can be correlated across the study area, but individual beds can not. Thinner skeletal packstone beds are often lensoidal and pinch out completely over 100's of ft (10's of m). In 2D outctops, skeletal packstone beds form a continuum of morphologies from isolated lenses to continuous pinch and swell beds (Fig. 8). Two skeletal packstone beds (26 and 30) change significantly across the study area (Fig. 9). Bed 30 in Antonio Creek consists of stacked, laterally discontinuous skeletal packstone lamina sets of 5–10 ft (2–3 m) hummocks and swales. Over 1000's of ft (100's of m) sever-

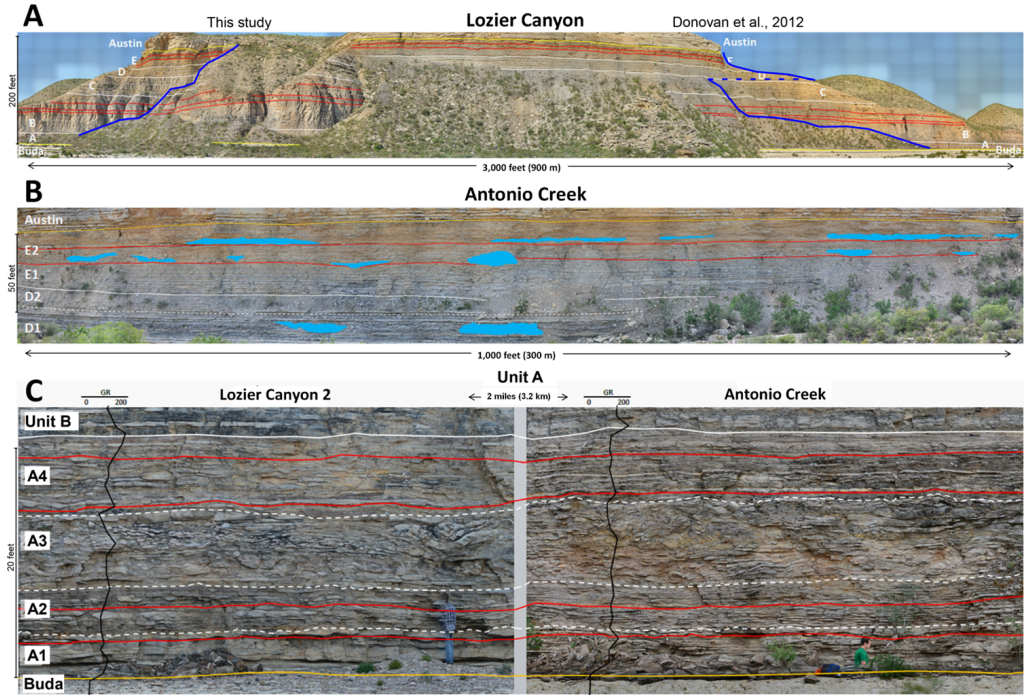

Figure 5. Annotated Gigapan photomosaics. Red lines represent bentonite beds, white solid lines are unit boundaries, dotted white lines are sub-unit boundaries, blue lines show the locations of measured sections, blue shapes mark the extent of deformed beds, and orange lines mark the boundaries with the underlying Buda Limestone and overlying Austin Chalk. (A) Lozier Canyon 1 outcrop. Note the location of measured sections. (B) Units D and E in Antonio Creek. Note the distribution of deformed zones. (C) A comparison of unit A at the Lozier Canyon 2 site and Antonio Creek.

Table 3. Description of units correlated in this study.

	A	B	C	D	E
Thickness					
Lozier Canyon	20.5 ft (6.2 m)	74.5 ft (22.7 m)	40.5 ft (12.3 m)	21 ft (6.4 m)	27.0 ft (8.2 m)
Antonio Creek	22.0 ft (6.7 m)	74.0 ft (22.6 m)	40.5 ft (12.3 m)	20.0 ft (6.0 m)	26.0 ft (7.9 m)
Lithology	1–12 in (3–30 cm) thick bed sets of skeletal packstone-grainstone interbedded with calcareous mudstone; thin <1 in (<3 cm) thick bentonite beds; abundant foraminifera, pellets, bivalves, echinoderm fragments, fish bones; locally common <0.5 in (<1 cm) ammonites, shark teeth, oysters, phosphatic grains, *Planolites*, *Chondrites*; rare gastropods, 3–20 in (8–50 cm) wood fragments; plesiosaur skeleton, framboidal pyrite; rare quartz silt	Very dark gray calcareous mudstone interbedded with skeletal packstone; <1–6 in thick (<3–15 cm) bentonite beds; abundant planktonic foraminifera, micrite clasts; common bivalves, fish bones; locally common *Planolites*; rare 5–10 in (13–25 cm) ammonites, <6 in (<15 cm) bony fish, unidentified large vertebrate skeleton, framboidal pyrite	Medium gray calcareous mudstone interbedded with 2–12 in thick (6–30 cm) beds sets of skeletal wackestone-packstone; thin <1 in (<3 cm) thick bentonite beds; abundant forams, bivalves, pellets, *Thalassinoides*, *Teichichnus*, *Taenidium*, *Planolites*, *Chondrites*, framboidal pyrite	1–8 in (3–20 cm) thick irregular layers and nodules of skeletal wackestone and packstone; bedding is burrow homogenized; interbedded calcareous mudstone; thin <1 in (<3 cm) thick bentonite beds; abundant foraminifera, pellets, bivalves, brachiopods, fish bones, echinoid *Hemiaster jacksonii*, unidentified ichnofossils; locally common 10–25 in (25–64 cm) ammonites, framboidal pyrite	1–12 in thick (3–30 cm) skeletal packstone and wackestone; interbedded calcareous mudstone; 1–8 in (3–20 cm) thick bentonite beds; abundant foraminifera, pellets, bivalves, brachiopods, fish bones, echinoid *Hemiaster jacksoni*, *Chondrites, Taenidium*, unidentified ichnofossils, framboidal pyrite
Sedimentary Structures	Abundant hummocky cross-stratification, wave ripples, combined flow ripples, fluid escape structures; soft sediment deformation; horizontal burrows	Abundant horizontal laminations, low-angle inclined laminations, cross stratification, horizontal burrows; locally common fluid escape structures	Abundant burrows, cross laminations; low-angle inclined laminations, ripple laminations	Abundant burrows; rare preserved cross stratified laminations in nodules	Abundant burrows; ripple laminations; cross stratification
Environment	Restricted shelf, within storm wave base; anoxic	Restricted shelf, episodically within storm wave base; anoxic	Open shelf, within storm wave base, oxic	Open shelf, within storm wave base, oxic	Open shelf, within storm wave base, oxic

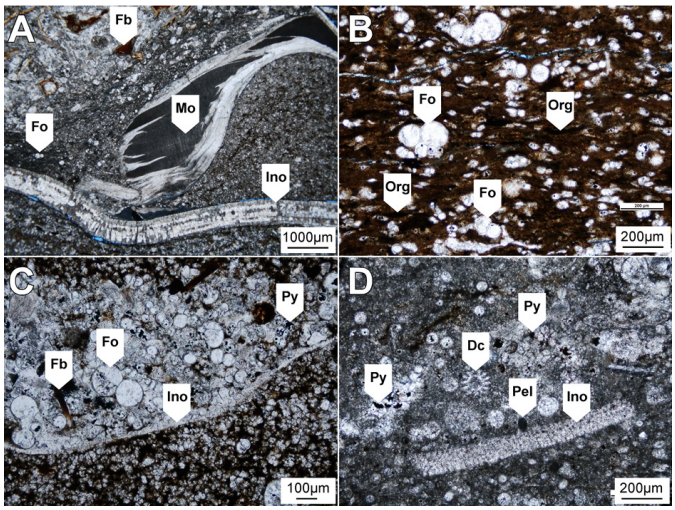

Figure 6. Photomicrographs containing planktonic foraminifera (Fo), fish bones (Fb), oysters (Mo), inoceramid bivalves (Ino), organic matter (Org), pyrite (Py), dasyclad algae (Dc), and peloids (Pel). (A) Skeletal grainstone in subunit A4. (B) Calcareous mudstone in unit B. (C) Skeletal packstone in unit B. (D) Skeletal packstone in unit D.

Table 4. Thickness of subunits in feet (meters).

Sub-unit	Lozier Canyon		Antonio Creek		ΔThickness
E2	16.0	(4.9)	13.5	(4.1)	15.6%
E1	10.0	(3.0)	13.5	(4.1)	35.0%
D2	8.5	(2.6)	9.0	(2.7)	5.9%
D1	12.5	(3.8)	11.0	(3.4)	12.0%
C3	5.5	(1.7)	3.5	(1.1)	36.4%
C2	21.0	(6.4)	20.5	(6.2)	2.4%
C1	14.0	(4.3)	16.0	(4.9)	14.3%
B5	9.0	(2.7)	10.0	(3.0)	11.1%
B4	11.5	(3.5)	13.5	(4.1)	17.4%
B3	26.0	(7.9)	26.5	(8.1)	1.9%
B2	18.0	(5.5)	16.0	(4.9)	11.1%
B1	10.0	(3.0)	8.0	(2.4)	20.0%
A4	7.0	(2.1)	6.5	(2.0)	7.1%
A3	7.0	(2.1)	8.0	(2.4)	14.3%
A2	3.5	(1.1)	4.5	(1.4)	28.6%
A1	3.0	(0.9)	3.0	(0.9)	0.0%

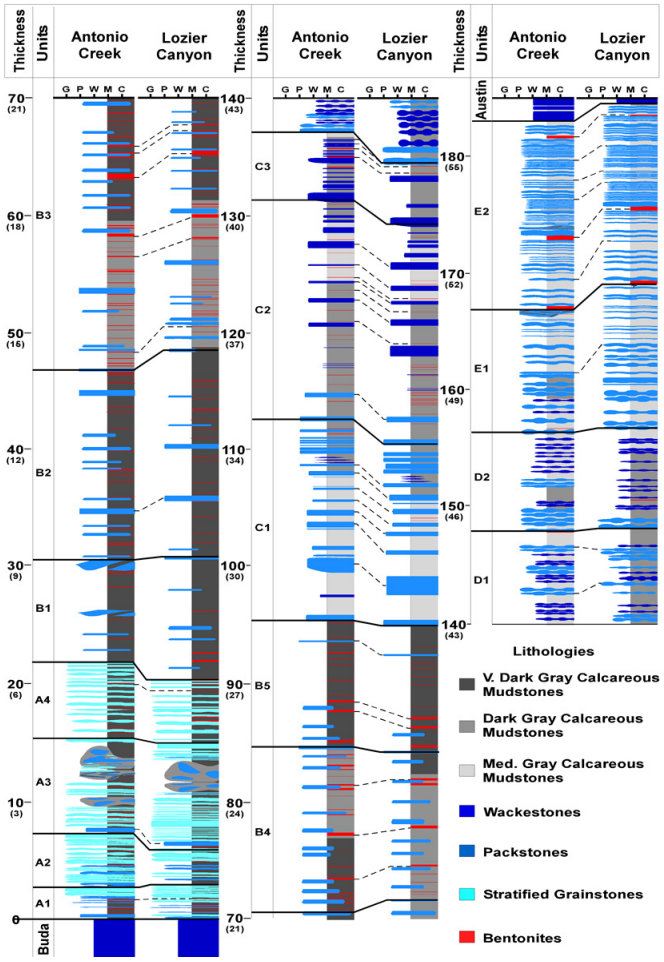

Figure 7. Comparison of lithologic data collected in Antonio Creek and Lozier Canyon. Solid black lines are unit boundaries. Dashed lines are confident correlations.

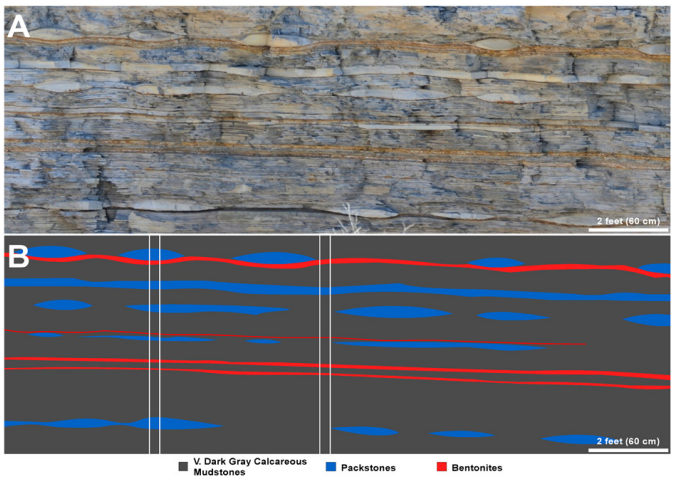

Figure 8. (A) Uninterpreted and (B) interpreted skeletal packstone beds in unit B showing a continuum of isolated lenses to continuous beds.

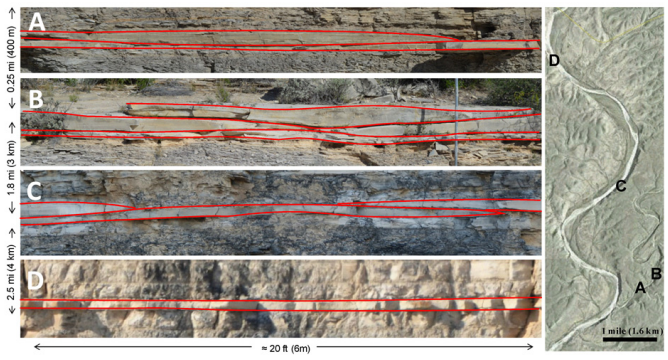

Figure 9. (A and B) Bed 30 in Antonio Creek. (C) Bed 30 at Lozier Canyon 2. (D) Bed 30 at the Lozier Canyon 1 outcrop.

al of these lamina sets pinch out completely and the bed consists of a single lamina set at the Lozier Canyon 1 site (Fig. 10). Bed 26 is similar to bed 30, but bed 26 is thinner and pinches out completely over about 1000 ft (300 m).

Skeletal packstone beds have consistent internal bedding features (low angle inclined laminations, horizontal laminations, wave ripples, small scale hummocky cross stratification, and current ripples) across the study area. Laterally continuous skeletal packstone beds tend to have have horizontal to lower angle laminations which transition to higher angles concomitant with the lateral change to discontinous isolated lenses.

Upper Eagle Ford

There is more consistent lateral continuity of individual beds within the Upper Eagle Ford formation across the study area (Fig. 10). There is significant variation in sub-unit C3 in Antonio Creek which contains an additional 2.5 ft (0.8 m) of dark gray calcareous mudstone below the contact with the overlying unit D in one location. The contact between units C and D contact is marked by rip-up clasts and is interpreted as the K70 sequence boundary. The nodular bedding of unit D is heavily bioturbated (BI:4–6) and lacks any preferred orientation in 3-D exposures (Fig. 11). Mudstone prone intervals contain discontinuous isolated nodules. Several thicker, laterally continuous correlative bedsets in unit D are correlative on all outcrops (Fig. 10). A discontinuous contorted zone occurs in sub-unit D1 with a lateral recurrence interval of 100's of ft (10's of m). Two major bentonites occurring in sub-unit E2 are visible on all the outcrops in the study area. In sub-unit E2, several well defined thickening upwards packages of ripple laminated packestone-grainstone beds are laterally continuous in the study area. Also in this unit are two discontinuous contorted zones with horizontal recurrence intervals of 10's of ft (3–10 m) (Fig. 5B). The contact with the Austin Chalk is abrupt and marked by rip-up clasts and is interpreted as the K72 sequence boundary (Donovan et al., 2012).

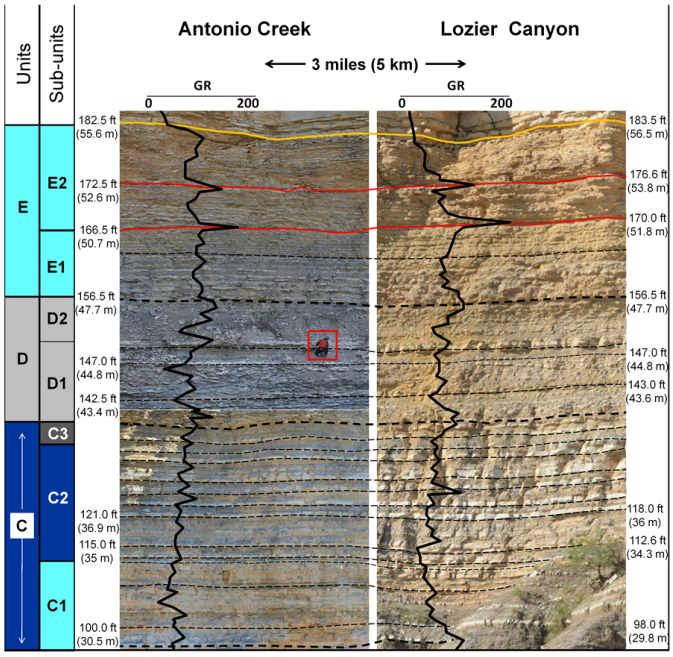

Figure 10. Lithologic correlation between resistant wackestone to packstone beds in the Upper Eagle Ford formation. The orange line marks the Eagle Ford–Austin Chalk boundary, red lines represent thick bentonites, black dashed lines represent facies (unit) boundaries, and thin black lines trace individual bed sets. The red box indicates a person on the outcrop for scale. The gamma ray kicks created by bentonite beds could be mistaken for condensed sections in the subsurface. Weathering may make the outcrops to appear more different than they really are. Fresh outcrop is accessible once the weathered surface is removed.

Figure 11. Nodular skeletal packstone-wackestone in subunit D1. Note the lack of preferred orientation. Vehicle for scale.

Spectral Gamma Ray Logs

SGR logs provide insight into the clay (K), bentonite (Th), and organic matter (U) enrichment profiles. In these sections K, Th, and U are lower within skeletal packstone and grainstone units and higher in mudstones and bentonites. The Upper Eagle Ford is noticeably richer in K and poorer in U than the Lower Eagle Ford formation. The SGR logs from each measured section have the same overall trends (Fig. 4), but not all peaks are correlative. The more notable differences are presented here. An increase in Th and U occurs at the top of sub-unit E2 just below the Austin Chalk contact in Antonio Creek and not in the Lozier Canyon log. There is an increase in K at the base of sub-unit B1 in Antonio Creek that does not occur in the other section. Th spikes appear to correspond directly with bentonite beds. There is a large Th spike at the base of sub-unit B1 that does not occur in Antonio Creek. Many other Th spikes are correlative but have higher values in Lozier Canyon than Antonio Creek, most notably in the Antonio Creek and Langtry members. Viewing the data in ternary diagrams (Fig. 12) highlights differences that are less noticeable on the logs like higher K values in unit D of Lozier Canyon.

DISCUSSION

Correlation of Units and Beds between Lozier Canyon and Antonio Creek

Measured sections in Lozier Canyon and Antonio Creek correlate very well. Similar thickness, sedimentary structures and SGR response occurs in most correlative beds. These strata correlate so well because the study area is relatively small and there was little or no depositional slope. The units correlated in this study correspond to four depositional sequences which have been correlated west into the subsurface of South Texas using biostratigraphic, electric log, geochemical, and core data (Donovan et al., 2012). The lack of lateral facies transition across the study area between these sequences supports their interpretation as unique chronostratigraphic units (e.g., unit C does not transition laterally into unit D, and unit E does not transition laterally into the Austin Chalk) at the scale of this study.

Correlating Spectral Wireline Logs

Excellent correlation between most trends and major peaks in gamma ray values between each section is not surprising given the similar lithology and proximity of the measured sec-

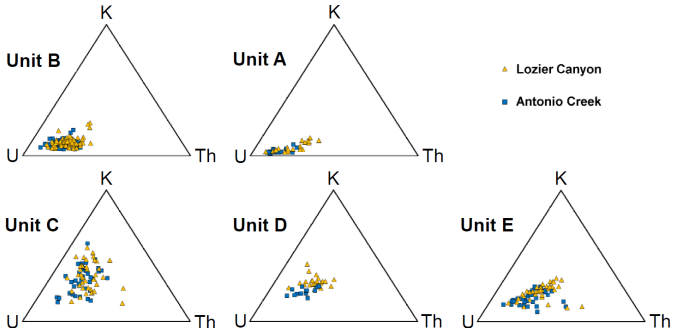

Figure 12. Ternary diagrams comparing the gamma ray readings within each unit from both canyons. Note the minor differences between clusters of the same unit in each canyon. These differences could be caused by errors in sampling or calibration.

tions. The differences in minor peaks between the two logs could easily be the result of the SGR sampling error described in the methods section of this paper. This may also be the case with the increase in uranium and thorium values in E2 just below the Austin Chalk contact in Antonio Creek. However, this difference could represent bentonites that has been eroded before deposition of the overlying Austin Chalk (K72 sequence) in Lozier Canyon. The variation in intensity of Th peaks between the two logs can also be attributed to sources of error issues previously described. Many of these differences might not exist if the same rocks were logged using a true downhole tool takes measurements continuously instead of at 1 ft (30 cm) intervals with a handheld device.

Th peaks increases significantly in sub-unit B3 concomitant with an abrupt increase in bentonite beds. U also increases in this interval; however the total gamma ray curve changes little. The underlying subfacies B2 has the highest total organic carbon (TOC) and is the primary completion target of some operators in the subsurface (Donovan et al., 2012) where it thickens stratigraphically. Greater accuracy in geosteering a well into this unit can be achieved by using MWD (measurement while drilling) systems that provide SGR data to distinguish between sub-units B2 and B3. This distinction would be problematic with only a total gamma ray curve. Another reason to use SGR data is that Th spikes from bentonites look like condensed sections on a total gamma ray curve of a well.

Water Depth and Depositional Slope during Deposition

The depth of water covering the platform during carbonate deposition of unit A in this area hinges on the interpretation of hummocky cross stratification (HCS). These structures (Fig. 13) of unit A along the U.S. Highway 90 and Lozier Canyon outcrops have been interpreted as either storm related structures (Trevino, 1988; Miller, 1990; Trevino and Smith, 2002; Donovan and Staerker, 2010; Donovan et al., 2012) or products of deeper water bottom currents, contourites, or turbidites (Lock and Peschier, 2006; Lock et al., 2010; Ruppel et al., 2012). The sedimentary structures (skeletal lags at the bases of beds, hummocky and swaley cross-stratification, and wave ripples) in Lozier Canyon and Antonio Creek outcrops are consistent with carbonate tempestites (Kreisa, 1981; Aigner, 1982; Tucker and Wright, 1990; Molina et al., 1997; Liu et al., 2012) and indicate shallow water deposition. The skeletal packstones in unit B contain sedimentary structures that also suggest shallow water deposition. This unit was probably periodically within storm wave base. The prevalence of wave related structures in the skeletal grainstone to packstone beds throughout the rest Eagle Ford Group in the study area suggest deposition within storm wave base.

Unit A is 7% thicker in Antonio Creek than in Lozier Canyon which could be the result of a higher sediment supply. Variation in the thickness and lateral continuity of individual beds in unit A is likely a natural result of deposition well within storm wave base. The lateral variation of skeletal packstone beds in unit B suggests differences in sediment supply or paleobathymetry during deposition (Fig. 14). The dominance of wave related structures within these beds suggests they were deposited within storm wave base. The carbonaceous mudstone facies contains primarily current related structures and may represent the background sedimentation which was periodically interrupted by large storms event which deposited the skeletal packstone beds. Any preexisting topography (Fig. 3B) on the Comanchee Platform may have been partially filled during deposition of unit A and B creating a flatter platform surface for subsequent deposition. This may explaining the higher incidence of correlative, laterally continuous beds in the Upper Eagle Ford formation and

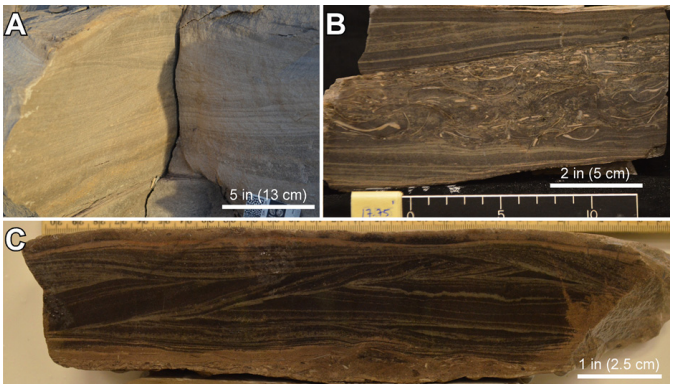

Figure 13. (A) HCS bed in sub-unit A1. (B) Shell lag in sub-unit A3. (C) A thin skeletal grainstone bed from sub-unit B3. Note the shell lag at the base, typical of shallow water storm deposits.

Figure 14. (A) A bed of stacked lamina sets. (B) A laterally continuous skeletal packstone pinch and swell bed. (C) Skeletal packstone lenses have an elongate disk tapered on the edges. The size of the bedforms are not to scale. The horizontal scale is accurate and is based on field observations.

the greater similarity in thickness and sedimentary structures of these beds across the study area.

Oxygenation of Bottom Waters

Adams and Weaver (1958) suggested that it was possible to infer chemical conditions during the deposition of sedimentary rocks based on Th and U concentrations in ash beds. In reducing conditions, the Th/U of ash beds would remain roughly constant because the U would not be scavenged or oxidized. If the ash had settled into oxidized waters, the U would have been oxidized and leached and thus the Th/U ratio would increase. They also noted that if Th and U were in zircons of the ash, the Th/U would be relatively impervious to leaching. In the study area, the bentonites in the Lower Eagle Ford formation have Th/U ratios of ≤1. In contrast, the bentonites in the Upper Eagle Ford formation have Th/U ratios between two and four suggesting more reducing conditions in the Lower Eagle Ford formation.

The value of U concentration as a proxy for reducing conditions is based on the findings of Hassan et al (1976) that higher concentrations of U tends to correlate with organic matter (TOC). However, as a number of workers have noted, U is susceptible to both pre-depositional and post-depositional weathering (Tribovillard et al 2006; Adams and Weaver 1958). To ensure that an interpretation of U for reducing conditions is valid, it can be compared with Mo. Molybdenum has the distinction of being an element that does not readily precipitate out of the water column, but its incorporation into sediments can be mediated by the presence of HS^- and scavenging by organics and Fe (McManus et al., 2006; Helz et al., 1996). This makes Mo a better proxy for inferring reducing conditions and thus if U and Mo data are in agreement, the concern of U leaching or mobilization is removed. Preliminary x-ray fluorescence (XRF) data collected at 6 in (15 cm) intervals in Antonio Creek reveal that U and Mo values strongly correlate (M. Wehner, 2013, personal communication). In this context, the higher U concentrations in the Lower Eagle Ford formation suggest greater preservation of organic matter and more reducing conditions than the Upper Eagle Ford formation which contains significantly lower U concentrations.

Bioturbation in the mudstone facies of the Lower Eagle Ford formation is rare but locally abundant *Chondrites* and *Planolites* occur in some skeletal packstones and grainstones. Bioturbation is common throughout all facies in the Upper Eagle Ford formation, including large vertical traces. The bioturbation index (BI) of the Lower Eagle Ford is between 0 and 1 and between 3 and 6 for the Upper Eagle Ford. The BI alone is not a reliable proxy for oxygen conditions. However, in conjunction with the geochemical data previously discussed, BI values recorded here serve to reinforce the interpretation of primarily anoxic and oxic conditions during deposition of the Lower and Upper Eagle Ford formations, respectively. The locally abundant ichnofossils in the skeletal packstone and grainstone facies in the Lower Eagle Ford formation could represent colonization by opportunistic organisms during periods of oxygenation following large storm events.

The pre-existing topography from the Comanchean buildups may have initially restricted circulation on the inner platform (Donovan et al., 2012) (Fig. 2B) resulting in the anoxic depositional conditions most prevalent in unit A and B (Lower Eagle Ford). Once the accommodation space from pre-existing topography was filled bottom circulation would have improved, explaining the upward increase in oxygen levels interpreted from the overall increase in widespread bioturbation and decrease in U beginning in unit C and prevalent throughout the rest of the Upper Eagle Ford.

Deformed Beds

Five contorted zones of deformed bedding occur in Antonio Creek (two in unit A and sub-units D1, E1, and E2) and three in Lozier Canyon (unit A and sub-units D1 and E2). These contorted zones show three similar styles of deformation. One type, usually near the base of a contorted zone, consists of clasts of laminated skeletal packstone-grainstone in a matrix or clast supported breccia (Fig. 15A). These beds were already firm when the deformation even occurred. Another style of deformation occurs as folded to overturned beds (Fig. 15B) and soft sediment deformation (Fig. 15C). The third style of deformation is represented by homogenized facies which bears no trace of the original depositional fabric (Fig. 15D), these commonly occur near the tops of the deformed horizons. These deformation styles likely correspond to the degree of lithification of the strata when deformation occurred. The contorted zones described in unit A along U.S. Highway 90 were attributed to debris flows (Lock and Peschier, 2006; Lock et al., 2010; Ruppel et al., 2012). The widespread, but laterally discontinuous nature of the deformed beds (Fig. 5B) suggests a more powerful, discontinuous mechanism produced them. The range of features from brittle to soft sediment deformation suggest that during deformation underlying beds became thixotropic and overlying beds sank into the underlying substrate and loose material was ejected into the water column and was deposited as massive bedding. Cyclic storm loading (Seilacher, 1984; Molina et al., 1998; Chen et al., 2009; Alfaro et al., 2002) and seismic shaking (Pope et al., 1997; Rosetti, 1999) were hypothesized to form similar structures. It is currently unclear which of these mechanisms formed the deformed beds in the Eagle Ford Group.

CONCLUSIONS

The minor variation in thickness and SGR logs of each unit across the study area indicates deposition occurred on a carbonate platform with little or no local depositional slope. Lateral variation of individual beds is greatest in units A and B. Bed thickness, external geometries, sedimentary structures, throughout the Eagle Ford section across the study area. Units within the four interpreted sequences (Donovan et al., 2012) do not transition laterally into units of overlying or underlying sequences. Geochemical and ichnofossil data suggest that depositional bottom waters were often anoxic during units A and B and oxic during units C, D, and E. Sedimentary structures suggest that deposition throughout the Eagle Ford Group in the study area occurred primarily above storm wave base. This suggests that deposition of successful unconventional plays like the Eagle Ford can occur in relatively shallow water. SGR data are necessary to accurately land horizontal wells in the highest TOC interval (subunit B2). Widespread deformed zones in the Eagle Ford Group may have been caused by cyclic storm loading or paleoseismicity.

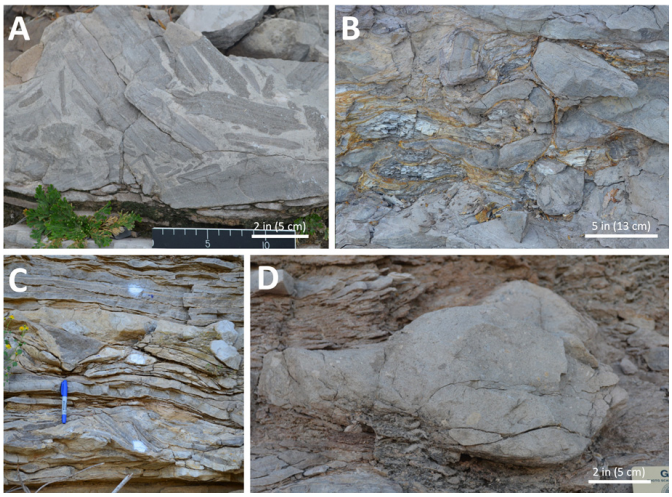

Figure 15. (A) This style of deformation forms a grainstone breccia. (B) Another style is characterized by overturned beds. (C) This style also contains soft sediment deformation. (D) The last style is completely homogenized skeletal packstone to grainstone beds.

ACKNOWLEDGMENTS

The authors are indebted to the reviewers of this manuscript (Tucker Hentz, Barry Katz, Bob Loucks, Robert Locklair, and Roger Slatt). BP America generously provided access to outcrops, financial, and logistical support for this project. Scott Staerker facilitated this study. Field assistance was generously provided by Nicole Gardner, Aris Pramudito, Abram Barker, and Bryce Gardner. The authors would like to thank Jacob Grosskopf for help identifying ichnofossils. This study was part of the senior author's Master's thesis. The senior author was supported by fellowships from the Berg-Hughes Center for Petroleum and Sedimentary Systems at Texas A&M University.

REFERENCES CITED

Adams, J. A. S., and C. E. Weaver, 1958, Thorium-to-uranium ratios as indicators of sedimentary processes: Examples of concept of geochemical facies: American Association of Petroleum Geologists Bulletin, v. 42, p. 387–430.

Aigner, T., 1982, Calcareous tempestites: Storm-dominated stratification in Upper Muschelkalk limestones (Middle Trias, SW Germany), *in* G. Einsele and A. Seilacher, eds., Cyclic and event stratification: Springer-Verlag, Berlin, Germany, p. 180–198, doi:10.1007/978-3-642-75829-4_13.

Alfaro, P., J. Delgado, A. Estevez, J. M. Molina, M. Moretti, and J. M. Soria, 2002, Liquefaction and fluidization structures in Messinian storm deposits (Bajo Segura Basin, Betic Cordillera, southern Spain): International Journal of Earth Sciences, v. 91, p. 505–513, doi:10.1007/s00531-001-0241-z.

Campbell, C. V., 1967, Lamina, lamina set, bed and bedset: Sedimentology, v. 8, p. 7–26, doi:10.1111/j.1365-3091.1967.tb01301.x.

Chen, J., S. K. Chough, S. S. Chun, and Z. Han, 2009, Limestone pseudoconglomerates in the Late Cambrian Gushan and Chaomidian formations (Shandong Province, China): Soft-sediment deformation induced by storm-wave loading: Sedimentology, v. 56, p. 1174–1195, doi:10.1111/j.1365-3091.2008.01028.x.

Donovan, A. D., and S. Staerker, 2010, Sequence stratigraphy of the Eagle Ford (Boquillas) Formation in the subsurface of South Texas and the outcrops of West Texas: Gulf Coast Association of Geologic Societies Transactions, v. 60, p. 861–899.

Donovan, A. D., T. S. Staerker, A. Pramudito, W. Li, M. J. Corbett, C. M. Lowery, A. M. Romero, and R. D. Gardner, 2012, The Eagle Ford outcrops of West Texas: A laboratory for understanding heterogeneities within unconventional mudstone reservoirs: Gulf Coast Association of Geological Societies Journal, v. 1, 162–185.

Droser, M. L., and D. J. Bottjer, 1986, A semiquantitive field classification of ichnofabrics: Journal of Sedimentary Petrology, v. 56, p. 558–559.

Dunham, R. J., 1962, Classification of carbonate rocks according to depositional texture, *in* W. E. Ham, ed., Classification of carbonate rocks—A symposium: American Association of Petroleum Geologists Memoir 1, p. 108–121.

Freeman, V. L., 1961, Contact of the Boquillas flags and Austin Chalk in Val Verde and Terrell counties, Texas: American Association of Petroleum Geologists Bulletin, v. 45, p. 105–107.

Freeman, V. L., 1968, Geology of the Comstock Indian Wells area Val Verde, Terrell, and Brewster counties, Texas: U.S. Geological Society Professional Paper 594–K, 26 p.

Harms, J. C., J. Southard, D. Spearing, and R. Walker, 1975, Depositional environments as interpreted from primary sedimentary structures and stratification sequences: Society of Economic Paleontologists and Mineralogists Short Course Notes 2, Tulsa, Oklahoma, 161 p.

Grabowski, G. J., 1995, Organic rich chalks and calcareous mudstone of the Upper Cretaceous Austin Chalk and Eagleford Formation, south-central Texas, USA, *in* B. J. Katz, ed., Petroleum source rocks: Springer-Verlag, Berlin, Germany, p. 209–234.

Hassan, M., A. Hossin, and A. Combaz, 1976, Fundamentals of the differential gamma ray log: Iinterpretation technique: Society of Professional Well Log Analysts Transactions, 17th Annual Logging Symposium, Paper 20.

Hazzard, R. T., 1959, Measured section, *in* R. L. Cannon, R. T. Hazard, A. Young, and K. P. Young, eds., 1986, Geology of the Val Verde Basin: West Texas Geological Society Guidebook, Midland, 118 p.

Helz, G. R., C. V. Miller, J. M. Charnock, J. F. W. Mosselmans, R. A. D. Pattrick, C. D. Gardner, and D. J. Vaughan 1996, Mechanism of molybdenum removal from the sea and its concentration in black shales: EXAFS evidence: *Geochima et Cosmochimica Acta*, v. 60, p. 3631–3642.

Hill, R. T., 1887b, The Texas section of the American Cretaceous: American Journal of Science, 3rd Series, v. 34, p. 287–309.

Kreisa, R. D., 1981, Storm-generated sedimentary structures in subtidal marine with examples from the Middle and Upper Ordovician of southwestern Virginia: Journal of Sedimentary Petrology, v. 51, p. 823–848, doi:10.1306/212F7DBF-2B24-11D7-8648000102C1865D.

Liu, X., J. Zhong, R. Grapes, S. Bian, and L. Chen, 2012, Late Cretacoues tempestite in northern Songliao Basin: China Journal of Asian Earth Sciences, v. 56, p. 33–41, doi:10.1016/j.jseaes.2012.02.007.

Lock, B. E., and L. Peschier, 2006, Boquillas (Eagle Ford) upper slope sediments, West Texas: Outcrop analogs for potential shale reservoirs: Gulf Coast Association of Geological Societies Transactions, v. 56, p. 491–508.

Lock, B. E., L. Peschier, and N. Whitcomb, 2010, The Eagle Ford (Boquillas Formation) of Val Verde County, Texas—A window on the South Texas play: Gulf Coast Association of Geological Societies Transactions, v. 60, p. 419–434.

McManus, J., W. M. Berelson, S. Severmann, R. L. Poulson, D. E. Hammond, G. P. Klinkhammer, and C. Holm 2006. Molybdenum and uranium geochemistry in continental margin sediments: Paleoproxy potential: *Geochima et Cosmochimica Acta*, v. 70, p. 4643–4662.

Miller, R. W., 1990, The stratigraphy and depositional environment of the Boquillas Formation of southwest Texas: M.S. thesis, University of Texas at Arlington, 156 p.

Molina, J. M., P. A. Ruiz-Ortiz, and J. A., Vera, 1997, Calcareous tempestites in pelagic facies (Jurassic, Betic Cordilleras, Southern Spain): Sedimentary Geology, v. 109, p. 95–109, doi:10.1016/S0037-0738(96)00057-7.

Molina, J. M., P. Alfaro, M. Moretti, and J. M. Soria, 1998, Soft-sediment deformation structures induced by cyclic stress of storm waves in tempestites (Miocene, Guadalquivir Basin, Spain): *Terra Nova*, v. 10, p. 145–150, doi:10.1046/j.1365-3121.1998.00183.x.

Pessagno, E. A., 1969, Upper Cretaceous stratigraphy of the western Gulf Coast area of Mexico, Texas, and Arkansas: Geological Society of America Memoir 111, Boulder, Colorado, 139 p.

Pope, M. C., J. F. Read, R. Bambach, and H. J. Hofmann, 1997, Late Middle to Late Ordovician seismites of Kentucky, southwest Ohio and Virginia: Sedimentary recorders of earthquakes in the Appalachian Basin: Geological Society of America Bulletin, v. 109, p. 489–503, doi:10.1130/0016-7606(1997)109<0489:LMTLOS>2.3.CO;2.

Reineck, H. E., and I. B. Singh, 1975, Depositional sedimentary environments, with reference to terrigenous clastics: Springer Verlag, New York, New York, 439 p.

Ruppel, S., R. Loucks, and G. Frébourg (leaders), 2012, Guide to field exposures of the Eagle Ford-equivalent Boquillas Formation and related Upper Cretaceous units in southwest Texas: Field seminar guidebook, 151 p.

Rosetti, D. F., 1999, Soft-sediment deformation structures in late Albian to Cenomanian deposits, Sao Luis Basin, northern Brazil: Evidence for palaeoseismicity: Sedimentology, v. 46, p. 1065–1081, doi:10.1046/ j.1365-3091.1999.00265.x.

Seilacher, A., 1984, Sedimentary structures tentatively attributed to seismic events: Marine Geology, v. 55, p. 1–12, doi:10.1016/0025-3227(84)90129-4.

Sloss, L. L., 1963, Sequences in the cratonic interior of North America: Geological Society of America Bulletin, v. 74, p. 93–114, doi:10.1130/0016-7606(1963)74[93:SITCIO]2.0.CO;2.

Smith, C. C., 1981, Calcareous nannoplankton and stratigraphy of late Turonian, Coniacian, and early Santonian age of the Eagle-Ford and Austin groups of Texas: U.S. Geological Society Professional Paper 1075, 96 p.

Treviño, R. H., 1988, Facies and depositional environments of the Boquillas Formation, Upper Cretaceous of southwest Texas: M.S. thesis, University of Texas at Arlington, 135 p.

Treviño, R. H., and C. I. Smith, 2002, Facies and depositional environments of the Boquillas Formation (abs.): American Association of Petroleum Geologists Annual Convention Program, v. 11, p. A177–A178.

Tribovillard, N., T. J. Algeo, A. Lyons, and A. Riboulleau, 2006, Trace metals as paleoredox and paleoproductivity proxies: An update: Chemical Geology, v. 232, p. 12–32.

Tucker, M. E., and V. P. Wright, 1990, Carbonate sedimentology: Blackwell Science, Ltd., Oxford, U.K., 482 p., doi:10.1002/9781444314175.

Winter, J. A., 1961, Stratigraphy of the Lower Cretaceous (subsurface) of South Texas: Gulf Coast Association of Geological Societies Transactions, v. 11, p. 15–24.